Spectroscopic Characterization of Precursors Used in the Pechini-Type Polymerizable Complex Processing of Barium Titanate

Masato Kakihana* and Momoko Arima

Materials and Structures Laboratory, Tokyo Institute of Technology, Nagatsuta 4259, Midori-ku, Yokohama 226-8503, Japan

Yoshiyuki Nakamura

Research Laboratory of Resources Utilization, Tokyo Institute of Technology, Nagatsuta 4259, Midori-ku, Yokohama 226-8503, Japan

Masatomo Yashima and Masahiro Yoshimura

Center for Materials Design, Materials and Structures Laboratory, Tokyo Institute of Technology, Nagatsuta 4259, Midori-ku, Yokohama 226-8503, Japan

Received September 22, 1998. Revised Manuscript Received November 30, 1998

Precursor solutions containing citric acid (CA), ethylene glycol (EG), and barium and titanium ions, previously used in the Pechini-type polymerizable complex (PC) processing of $BaTiO_3$, have been extensively characterized by Raman and ^{13}C NMR spectroscopy. The simultaneous presence of Ba and Ti ions has brought about the unusual dissociation of proton from the alcohol OH group of CA, thereby creating an alkoxide oxygen atom with a strong nucleophilic nature, which prompts rearrangement of CA to form a barium−titanium mixed-metal CA complex with a stoichiometry close to Ba/Ti/CA = 1:1:3. The solution spectroscopy data have been compared with those obtained for an isolated mixed-metal CA complex from a solution with a chemical formula of $BaTi(C_6H_6O_7)_3{\cdot}4H_2O$. The Raman spectrum of $BaTi(C_6H_6O_7)_3{\cdot}4H_2O$ has shown that the two terminal COOH groups of each CA coordinate in a monodentate fashion either to Ba or to Ti, while the central COOH group is not coordinating. The solid-state ^{13}C NMR spectrum of the same complex has indicated that the alcohol OH in CA is fully deprotonated to form an alkoxide oxygen atom, in agreement with the solution ^{13}C NMR data. A proposed model for the coordination structure of $BaTi(C_6H_6O_7)_3$ species, inferred from all these spectroscopic data, has displayed the presence of three fused six-memberd chelate rings arising from the full alkoxylation of CA ligands.

Introduction

Organic polymer precursors are often utilized in the synthesis of multicomponent oxide powders.[1−4] One of the most widely used polymeric routes is the so-called "polymerizable complex (PC)" method,[5] known originally as the Pechini process,[1] wherein a mixed solution of citric acid (CA), ethylene glycol (EG), water, and the desired metal cations is polymerized to form a polyester-type resin. The potential ability of CA to solubilize a wide range of metal cations in a mixed solvent of EG and H_2O is of prime importance, especially for systems involving cations that can be readily hydrolyzed to form insoluble precipitates in the presence of water. For example, the Pechini-type PC method can circumvent the problem of preferential precipitation of titanium compounds from aqueous media due to spatial fixation of water-resistant titanium−CA complexes in the resin. With this reason, a number of titanates with the general formula of $MTiO_3$ or $M_2Ti_2O_7$ have been successfully prepared at reduced temperatures by the Pechini-type PC method.[6−19] However, our knowledge of the molec-

* To whom all correspondence should be addressed. E-mail: kakihana@rlem.titech.ac.jp.

(1) Pechini, M. *P. U.S. Pat.* **1967**, *330* (3) , 697.
(2) Eror, N. G.; Anderson, H. U. In *Better Ceramics Through Chemistry II* Materials Research Society Proceedings; Brinker, C. J., Clark, D. E., Ulrich, D. R., Eds.; Materials Research Society, 1986; Vol. 73, p 571..
(3) Anderson, H. U.; Pennell, M. J.; Guha, J. P. In *Advances in Ceramics*: *Ceramic Powder Science*; Messing, G. L., Mazdiyasni, K. S., McCauley, J. W., Harber, R. A., Eds.; American Ceramic Society: Westerville, OH, 1987; p 91.
(4) Lessing, P. A. *Am. Ceram. Soc. Bull.* **1989**, *168*, 1002.
(5) Kakihana, M. *J. Sol−Gel Sci. Technol.* **1996**, *6*, 7.
(6) Budd, K. D.; Payne, D. A. In *Better Ceramics Through Chemistry I*, Materials Research Society Symposium Proceedings; Brinker, C. U., Clatk, D. E., Ulrich, D. R.; Elsevier: Pittsburgh, PA, 1984; p 239.
(7) Cho, S. G.; Johnson P. F.; Condrate, R. A., Jr. *J. Mater. Sci.* **1990**, *25*, 4738.
(8) Peschke, S. L.; Ciftcioglu, M.; Doughty, D. H.; Voigt, J. A. *Mater. Res. Soc. Symp. Proc.* **1992**, *271*, 101.
(9) Leite, E. R.; Sousa, C. M. G.; Longo, E.; Varela, J. A. *Ceram. Int.* **1995**, *21*, 143.
(10) Leite, E. R.; Varela, J. A.; Longo, E.; Paskocimas, C. A. *Ceram. Int.* **1995**, *21*, 153.
(11) Kakihana, M.; Okubo, T.; Arima, M.; Nakamura, Y.; Yashima, M.; Yoshimura, M. *J. Sol−Gel Sci. Technol.* **1998**, *12*, 95.

10.1021/cm9806681 CCC: $18.00
Published on Web 01/20/1999

Table 1. Molar Ratio of Ba/Ti/CA/EG in Solutions Used for Spectroscopic Characterization and the Approximate Description of Their Molecular Constitution

solution	Ba	Ti	CA	EG	approximate description of molecular constitution
BT0	0	0	1	4	no complex formation
BT1	0.1	0.1	1	4	$0.1BaTi{-}CA_3 + 0.7CA$
BT2	0.2	0.2	1	4	$0.2BaTi{-}CA_3 + 0.4CA$
BT3	0.3	0.3	1	4	$0.3BaTi{-}CA_3 + 0.1CA$
T1	0	0.1	1	4	$0.1Ti{-}CA_x + (1 - 0.1x)CA$
T2	0	0.2	1	4	$0.2Ti{-}CA_x + (1 - 0.2x)CA$
T3	0	0.3	1	4	$0.3Ti{-}CA_x + (1 - 0.3x)CA$
T4	0	0.4	1	4	$0.4Ti{-}CA_x + (1 - 0.4x)CA$
B2	0.2	0	1	4	$0.2Ba{-}CA_y + (1 - 0.2y)CA$
B1T3	0.1	0.3	1	4	$0.1BaTi{-}CA_3 + 0.2Ti{-}CA_x + (0.7 - 0.2x)CA$
B2T3	0.2	0.3	1	4	$0.2BaTi{-}CA_3 + 0.1Ti\text{-}CA_x + (0.4 - 0.1x)CA$
B2T1	0.2	0.1	1	4	$0.1BaTi{-}CA_3 + 0.1Ba\text{-}CA_y + (0.7 - 0.1y)CA$
B3T1	0.3	0.1	1	4	$0.1BaTi{-}CA_3 + 0.2Ba{-}CA_y + (0.7 - 0.2y)CA$

ular constitution of precursor solutions used in the Pechini-type PC processing is quite limited, although a basic understanding of the precursor solution chemistry by means of appropriate spectroscopic techniques would be quite a useful approach for the subsequent establishment of optimum preparative conditions and thus could allow a better control of the properties of the resulting oxide material.

We report here the results of the investigations of the Ba−Ti−CA−EG−(H_2O) system, which has been used as a precursor solution for the low-temperature synthesis of $BaTiO_3$.[12−16] Previously reported characterization data for Ba/Ti/CA/EG precursor solutions were obtained mainly by ^{13}C NMR spectroscopy,[16] from which some pertinent information was provided regarding the type of complexes formed in solutions, in particular, the possible presence of a mixed-metal (Ba,Ti)−CA_3 complex in EG postulated by the authors[16] being very important, since formation of such a mixed-metal complex with the correct stoichiometry is crucial to control over the stoichiometry and homogeneity of the final $BaTiO_3$ material. However, the ratio of Ba to Ti in the proposed mixed-metal complex still remains somewhat unclear. The primary goal of this paper is therefore to obtain further insight into the molecular constitution of precursors used in the Pechini-type PC processing of $BaTiO_3$ by using Raman and ^{13}C NMR spectroscopic techniques. The solution spectroscopic data obtained in this work will then be compared with those for an isolated mixed-metal citrate from an aqueous solution with a chemical formula close to $BaTi(C_6H_6O_7)_3{\cdot}4H_2O$. Finally, a possible model for the coordination structure of $BaTi(C_6H_6O_7)_3$ speceis, inferred from all these spectroscopic data, will be proposed.

Experiment

(1) Preparation and Characterization of CA/EG Solutions with Various Amounts of Ba and Ti Ions. Barium carbonate ($BaCO_3$), titanium tetraisopropoxide (Ti[OCH-$(CH_3)_2]_4$ = Ti($O^iPr)_4$), anhydrous CA ($HOOCCH_2C(OH)$−$(COOH)CH_2COOH$), and EG ($HO{-}CH_2CH_2{-}OH$) were used as starting chemicals. The molar ratio of CA/EG was kept at 1:4 for all the solutions used, and 0.1−0.4 mol of metals with respect to 1 mol of CA were dissolved in the CA/EG solution. The reference solution of CA/EG without Ba and Ti ions is designated as "BT0", while those containing, for instance, (1) 0.2 mol of Ba + 0.2 mol of Ti and (2) 0.3 mol of Ba + 0.1 mol of Ti are designated as "BT2" and as "B3T1", respectively. Table 1 lists the molar ratio of Ba/Ti/CA/EG for each solution used for the present study, together with the approximate description of the molecular constitution (discussed later). A typical preparation scheme is given below for the solution of "B3T2" as an example. An amount of 0.2 mol of Ti($O^iPr)_4$ was dissolved in 4 mol of EG followed by addition of 1 mol of CA. A transparent solution was obtained after the mixture was stirred at ~40 °C for 2 h. Then 0.3 mol of $BaCO_3$ was added, and the mixture was stirred at ~60 °C for 4 h until it became transparent.

A standard Raman spectrometer (model T64000, Jobin Yvon/Atago Bussan, France/Japan) equipped with a liquid nitrogen cooled CCD (charge-coupled device) detector was used in a conventional macrobeam setup with a 90° scattering geometry. The 515 nm line of an Ar laser was used as an excitation source. ^{13}C NMR {^1H} (decoupled) spectra were recorded using a standard Fourier transform NMR spectrometer (JEOL, NMR-GSX-270, Japan) operating at 67.9 MHz of a ^{13}C resonance frequency. The sample solutions were transferred to a 10 mm diameter NMR tube, and inside this tube was coaxially placed a 2 mm diameter capillary tube containing a deuterated lock solvent (D_2O). Tetramethylsilane (TMS) was used as a reference for reported ^{13}C chemical shifts, i.e., the resonance position of the methyl carbon of TMS being set to 0 ppm.

(2) Isolation and Characterization of a Mixed Ba−Ti Citric Acid Complex. The isolation of a mixed Ba−Ti CA complex followed the previously reported procedure[20−22] with some modifications, as shown in Figure 1. Titanium *n*-buthoxide (Ti(O-^{n}Bu)$_4$) was added to an aqueous solution of CA (2.5 mol/L) with a molar ratio of CA/Ti = 2:1 and was stirred at room temperature for 3 h until a milky colloidlike solution was obtained. The pH of the solution was adjusted to 5 by addition of ammonia, as a result of which the milky colloidlike solution became transparent. Barium carbonate was added to another aqueous solution of CA (2.5 mol/L) with a molar ratio of CA/Ba = 4:1. The Ti−CA solution was then added to the Ba−CA solution with continuous stirring followed by addition of HCl to pH = 2. After about 2 h under stirring a mixed Ba−Ti CA complex precipitated out. It was filtered, washed with aqueous HCl solution of pH 2 several times, and finally dried at 80 °C for 3 h in an oven. The resulting compound was a white powder.

(12) Kumar, S.; Messing, G. L. *Mater. Res. Soc. Symp. Proc.* **1992**, *271*, 95.
(13) Kumar, S.; Messing, G. L.; White, W. *J. Am. Ceram. Soc.* **1993**, *76*, 617.
(14) Kumar, S.; Messing, G. L. *J. Am. Ceram. Soc.* **1994**, *77*, 2940.
(15) Arima, M.; Kakihana, M.; Yashima, M.; Yoshimura, M. *Eur. J. Solid State Inorg. Chem.* **1995**, *32*, 863.
(16) Arima, M.; Kakihana, M.; Nakamura, Y.; Yashima, M.; Yoshimura, M. *J. Am. Ceram. Soc.* **1996**, *79*, 2847.
(17) Kakihana, M.; Okubo, T.; Arima, M.; Uchiyama, O.; Yashima, M.; Yoshimura, M.; Nakamura, Y. *Chem. Mater.* **1997**, *9*, 451.
(18) Kakihana, M.; Milanova, M. M.; Arima, M.; Okubo, T.; Yashima, M.; Yoshimura, M. *J. Am. Ceram. Soc.* **1996**, *79*, 1673.
(19) Milanova, M. M.; Kakihana, M.; Arima, M.; Yashima, M.; Yoshimura, M. *J. Alloys Compd.* **1996**, *242*, 6.
(20) Mulder, B. J. *Ceram. Bull.* **1970**, *49*, 990.
(21) Hennings, D.; Mayr, W. *J. Solid State Chem.* **1978**, *26*, 329.
(22) Hutchins, G. A.; Maher, G. H.; Ross, S. D. *Ceram. Bull.* **1987**, *66*, 681.

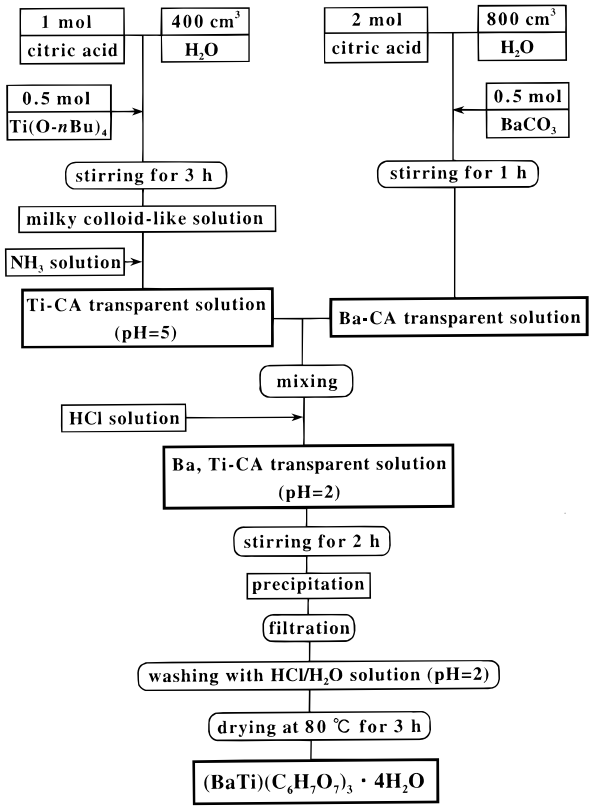

Figure 1. Flowchart for obtaining a mixed-metal complex with a chemical formula of $BaTi(C_6H_6O_7)_3 \cdot 4H_2O$.

The Ba and Ti contents in the Ba−Ti CA complex were determined, after dissolving the complex in a concentrated HCl aqueous solution, by a standard ICP (inductively coupled plasma) analysis. The C, H, and O content in the Ba−Ti CA complex were determined by quantifying its gaseous decomposition products (H_2O and CO_2) at 1000 °C using a standard elemental analysis equipment (Perkin-Elmer, 2400IICHNS/O). The thermal decomposition of the Ba−Ti CA complex was studied by means of TG-DTA/MS (MAC Science, thermogravimetry-differential thermal analysis/mass spectrometry system) at a heating rate of 40 °C/min and X-ray diffraction (XRD) using Cu Kα radiation (MAC Science, MXP3VA) with a scan rate of 4° (2θ)/min. Solid-state ^{13}C NMR spectra were recorded on a JEOL NMR-GSX-270 spectrometer operating at 67.9 MHz using a cross-polarization magic angle spinning (CP-MAS) technique. The chemical shifts were externally referenced to adamantan ($C_{10}H_{16}$), but the reported values were rescaled by the TMS standard for the sake of convenience.

The Raman spectra in the range 200−1800 cm^{-1} were measured with the 514 nm line of an Ar laser in a backscattering geometry using microprobe optics (Atago Bussan Co.). The laser beam was focused onto the sample surface with a 90× objective lens to a spot of several micrometers in diameter. The scattered light was analyzed with a Jobin-Yvon T64000 triple spectrometer and collected with a CCD detector.

A possible model for the coordination structure in the Ba−Ti CA complex inferred from all these spectroscopic data was proposed, and positions of each atom were optimized by a standard molecular mechanics calculation using a commercially available software "Mechanics" (CAChe Science Co.).

Results and Discussion

(1) Solution Characterization by Raman and ^{13}C NMR Spectroscopy. *(a) Raman Spectroscopy.* Spectra a−d of Figure 2 respectively show Raman spectra of BT0, B2, T2, and BT2. A great similarity of the Raman spectrum of B2 (Figure 2b) and BT0 (Figure 2a) suggests

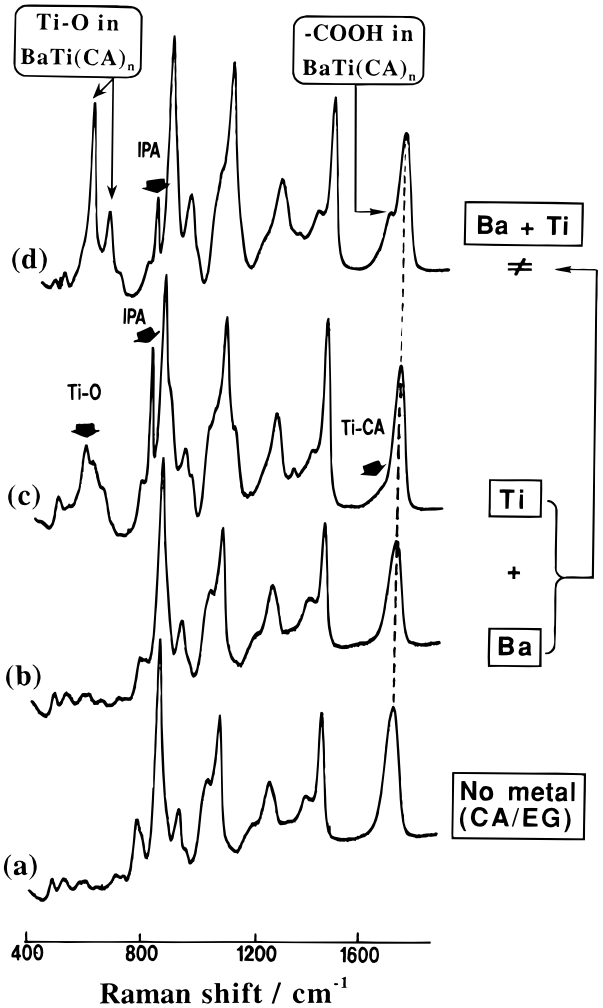

Figure 2. Raman spectra of various solutions with the molar ratio Ba/Ti/CA/EG = (a) 0:0:1:4 (BT0), (b) 0.2:0:1:4 (B2), (c) 0:0.2:1:4 (T2), and (d) 0.2:0.2:1:4 (BT2).

a weak interaction between barium ions and CA in accordance with the low stability constants for Ba−CA complexes.[23] In contrast, there have been at least three substantial changes in the Raman spectra of T2 and BT2 when compared with the Raman spectrum of the reference sample BT0.

(i) A characteristic Raman peak of "free" isopropyl alcohol (^{i}PrOH) near 820 cm^{-1} (marked as "IPA" in spectra c and d of Figure 2) showed up, while no Raman peaks corresponding to isopropoxides in $Ti(O^iPr)_4$ were observed. This observation strongly suggests a ligand-exchange reaction between $Ti(O^iPr)_4$ and CA, written by the following type of equation:

$$Ti(O^iPr)_4 + 2CA{-}(COOH)_3 \rightarrow Ti[CA(COO)_2(COOH)]_2 + 4^iPrOH \quad (1)$$

(ii) New strong Raman peaks showed up near 600 cm^{-1}, which can be assigned to Ti−O stretching vibrational modes in CA complexes.[16,24] Note, however, that the shape of the 600 cm^{-1} Raman bands of BT2 differs considerably from that of T2. This suggests that the

(23) Pearce, K. N. *Aust. J. Chem.* **1980**, *33*, 1511.
(24) Payne, M. J.; Berglund, K. A. *Mater. Res. Soc. Symp. Proc.* **1986**, *73*, 571.

molecular constitution of BT2 with respect to the bonding fashion of Ti−O is significantly different from that of T2 as discussed extensively later. Spectra a−e of Figure 3 respectively show Raman spectra of BT0, T1, T2, T3, and T4. The intensity of the characteristic 600 cm^{-1} Ti−O bands is monotonically increased with increasing the titanium concentration, just indicating a linear increase in the mole fraction of the Ti−CA complex formed through the eq 1. Similarly, the intensity of the other characteristic 600 cm^{-1} Ti−O bands observed for solutions containing both Ba and Ti in equal amounts is increased simply with an increase of the Ba/Ti content as shown in spectra a−d of Figure 4, where the Raman spectra of BT0, BT1, BT2, and BT3 are displayed, respectively.

(iii) The characteristic band at 1730 cm^{-1} assigned to the carbonyl stretching mode in the −COOH carboxylic acid groups of CA[25,26] was significantly modified by the appearance of a distinct shoulder in the lower frequency region, suggesting a strong interaction of titanium ions with carboxylic acid groups of CA. The behavior of the shoulder near 1630 cm^{-1} is basically similar to what has been observed for the characteristic 600 cm^{-1} Ti−O bands, i.e., the shape of the shoulder of BT2 differing from that of T2 (Figure 2d vs Figure 2c) and the intensity of each individual shoulder being increased monotonically with increasing metal content (Figures 3 and 4).

An important observation worthy to be stressed here is that the Raman spectrum of (Ba,Ti)−CA/EG cannot be interpreted in terms of a simple superposition of the individual Ba−CA/EG and Ti−CA/EG Raman spectra; i.e., [the spectrum of B2] + [the spectrum of T2] is not equal to [the spectrum of BT2], as shown in the right-hand side of Figure 2. This would in turn indicate that Ba and Ti cations have a strong interaction during the chelation, presumably to form a mixed-metal CA complex that should be different from the Ti−CA complex described in eq 1. Our supposition is then that a mixed-metal CA complex with a stoichiometric ratio of Ba/Ti = 1:1, $BaTi{-}CA_n$, forms as a predominant complex species in CA/EG solutions containing both Ba and Ti ions in equal amounts. To testify this hypothesis, Raman spectra of CA/EG solutions containing Ba and Ti ions in unequal amounts were measured. Spectra a−e of Figure 5 respectively show Raman spectra of BT0, T3, B1T3, B2T3, and BT3. The Raman spectrum of B1T3 (Figure 5c) can be basically described as a simple combination of those characteristic for the BT1 (Figure 4b) and T2 (Figure 3c) solutions. Similarly, the Raman spectrum of B2T3 (Figure 5d) can be interpreted in terms of a simple superposition of the two Raman spectra of BT2 (Figure 4c) and T1 (Figure 3b). These observations indicate that the molecular constitution of B1T3 and B2T3 solutions can be described as mixtures of $BaTi{-}CA_n$ and Ti−CA complexes with molar ratios of 1:2 and 2:1, respectively, i.e., the excess Ti giving rise to no substantial effect on the metal stoichiometry of the mixed-metal $BaTi{-}CA_n$ complex. It is thus plausible that the simultaneous presence of Ba and Ti ions in CA/EG solutions produces a mixed-metal $BaTi{-}CA_n$ complex with a stoichiometric Ba/Ti = 1 ratio. The conclusion drawn from the Raman spectroscopic data is further substantiated by measuring the ^{13}C NMR spectra of these solutions, the results of which are shown in the next section.

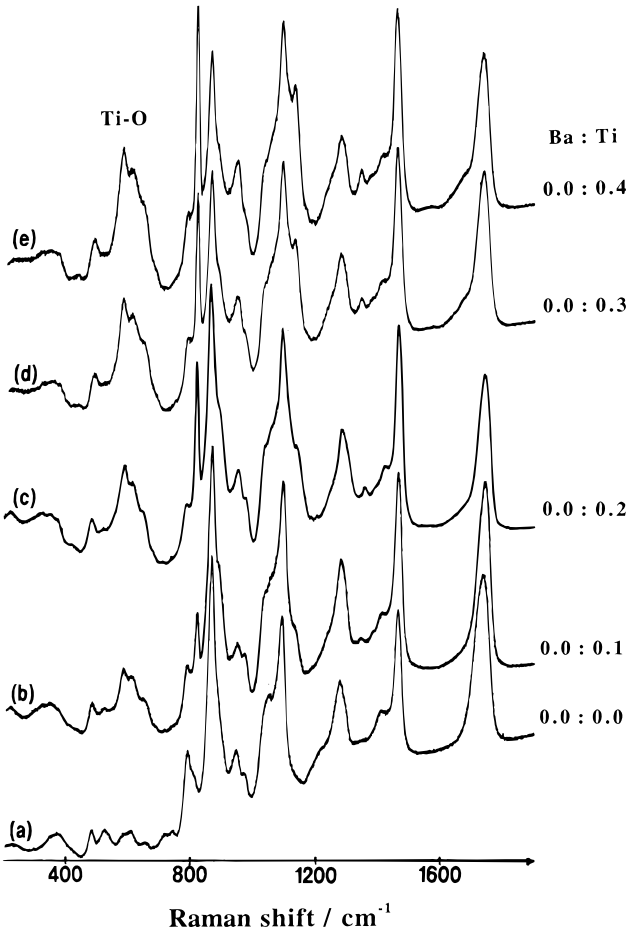

Figure 3. Raman spectra of various solutions with the molar ratio Ba/Ti/CA/EG = (a) 0:0:1:4 (BT0), (b) 0:0.1:1:4 (T1), (c) 0:0.2:1:4 (T2), (d) 0:0.3:1:4 (T3), and (e) 0:0.4:1:4 (T4).

(b) ^{13}C NMR Spectroscopy. Spectra a−d of Figure 6 respectively show $^{13}C\{^1H\}$ NMR (decoupled) spectra of BT0, B2, T2, and BT2 in two selected regions of 20−95 ppm (Figure 6A) and 170−190 ppm (Figure 6B). For the sake of convenience, Scheme 1 shows the assignment of some NMR peaks to certain carbon centers. Each carbon center in CA or EG is defined at the top of Scheme 1, while carbon centers in some derivatives as a result of esterfication reactions between CA and EG are defined as the bottom two structures of Scheme 1.

The $^{13}C\{^1H\}$ NMR spectrum of CA/EG (spectrum a of Figure 6A and spectrum a of Figure 6B) shows a rather complicated feature compared to what is expected from a simple mixture of CA and EG. The expected number of $^{13}C\{^1H\}$ NMR signals for CA and EG in solution should be four (carbons a−d) and one (carbon e), respectively. Since esterification between the hydroxyl OH group of EG and the carboxylic acid COOH group of CA occurs gradually during the dissolution process of CA into EG,[5] some extra peaks due to carbon centers of a_1, b_1, c_1, d_1, e_1, and e_2 (as defined in Scheme 1) were observed in addition to the main resonances due to carbon centers a−e for nonesterificated CA and EG.

(25) Bellamy, L. J. *The Infrared Spectra of Complex Molecules*; Chapman and Hall: London, 1975; pp 176−179.
(26) Tarakeshwar, P.; Manogran, *S. Spectrochim. Acta* **1994**, *50A*, 2327.

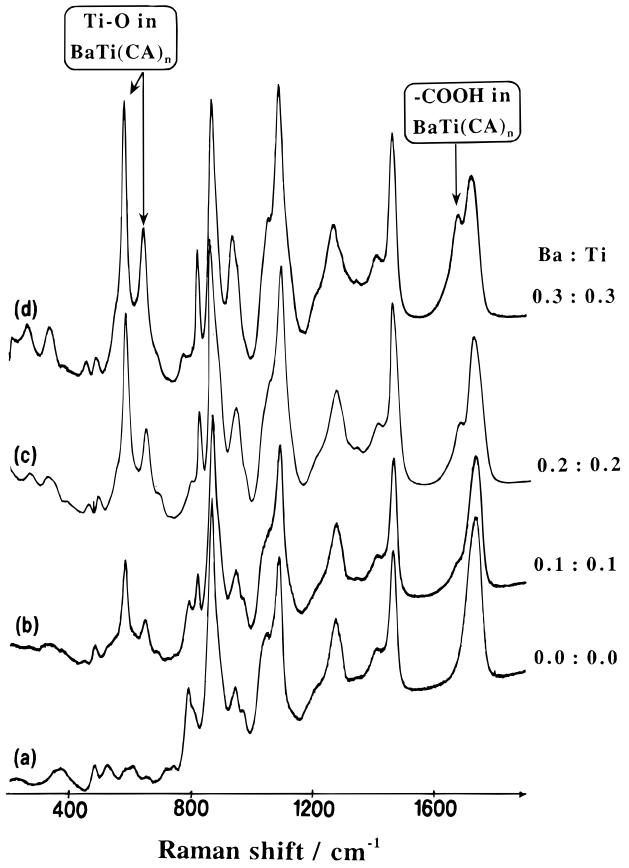

Figure 4. Raman spectra of various solutions with the molar ratio Ba/Ti/CA/EG = (a) 0:0:1:4 (BT0), (b) 0.1:0.1:1:4 (BT1), (c) 0.2:0.2:1:4 (BT2), and (d) 0.3:0.3:1:4 (BT3).

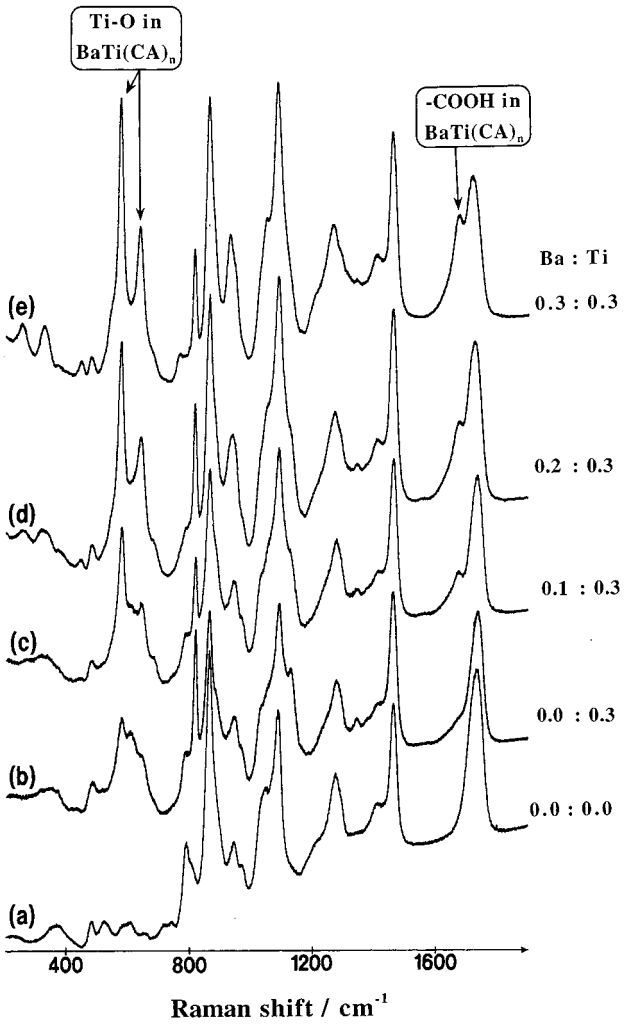

Figure 5. Raman spectra of various solutions with the molar ratio Ba/Ti/CA/EG = (a) 0:0:1:4 (BT0), (b) 0:0.3:1:4 (T3), (c) 0.1:0.3:1:4 (B1T3), (d) 0.2:0.3:1:4 (B2T3), and (e) 0.3:0.3:1:4 (BT3).

Scheme 1

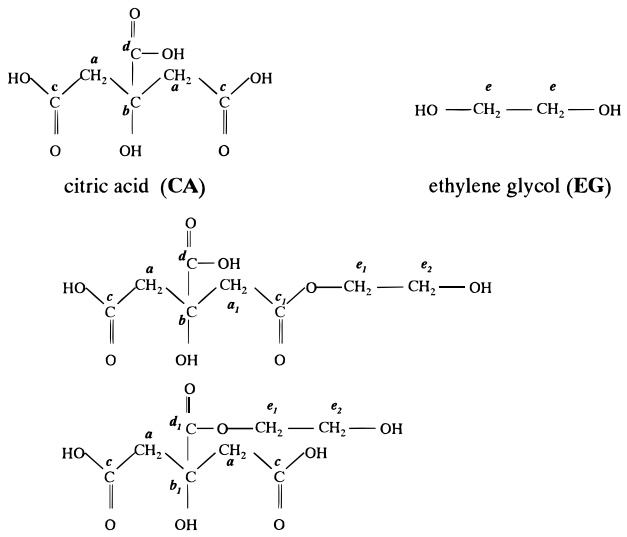

There still remain some weak extra peaks that cannot be explained by Scheme 1. They can be assigned to carbon centers of a number of diester or even of higher order ester products with similar structures. The largest degree of esterification occurred for the CA/EG solution without metals (see spectrum a of Figure 6A), while a smaller degree of esterification occurred for solutions containing Ti ions (see spectra c and d of Figure 6A). This indicates a decreased number of free CA due to the complexation between CA and Ti ions in solutions containing Ti ions. Another factor that affects the degree of esterification involves the different duration of the time required for preparing solution samples; i.e., when the dissolution of CA and metal compounds ($BaCO_3$ and/or $Ti(O-^iPr)_4$) into EG takes longer time, the degree of esterification is increased. Although the esterification between CA and EG complicates the full interpretation of the ^{13}C NMR spectra, we believe that it does not seriously influence the basic scheme for formation of metal CA complexes. This is because all the solutions tested involve excess CA for complex formation, and hence, the complex formation between CA and metals can be completed before most of CA are consumed for esterification reactions. It is probable that esterification occurs between EG and free CA not bonded to metals, since once carboxylic acid groups of CA are incorporated into the complex formation, they can no longer participate in esterification reactions. Turning back to Figure 6A, the methylene resonance of CA (~46 ppm; peak a) is now used as an internal standard for estimation of integrated intensities in different samples throughout this study, since it is well separated from other resonances and since methylene carbons even in esterificated CA (e.g., peak a_1) have chemical shifts similar to that of nonesterificated CA so that we can count all the

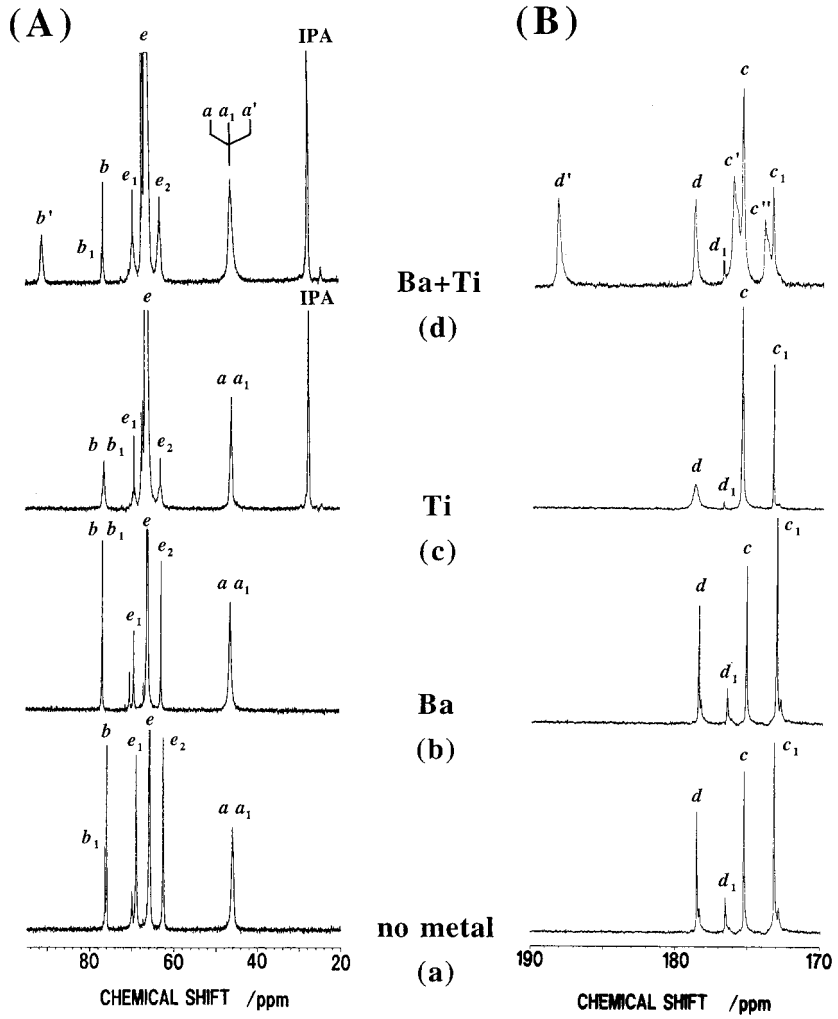

Figure 6. $^{13}C\{^1H\}$ NMR (decoupled) spectra in two representative regions of (A) 20−94 pm and (B) 170−190 ppm for various solutions with the molar ratio Ba/Ti/CA/EG = (a) 0:0:1:4 (BT0), (b) 0.2:0:1:4 (B2), (c) 0:0.2:1:4 (T2), and (d) 0.2:0.2:1:4 (BT2). IPA stands for isopropyl alcohol. For definition of other symbols marked on peaks, see Schemes 1−3 as well as the text.

intensities corresponding to the initially known amount of CA without omission.

One of the most striking results is that the simultaneous presence of Ba and Ti ions in the CA/EG solution gives rise to two new resonances at 91 ppm (b′) and 188 ppm (d′) in addition to the resonances at 77 ppm (b) and 178 ppm (d) associated with the alcoholic and carboxylic acid carbons of CA (spectrum d of Figure 6A and spectrum d of Figure 6B), which in turn indicates that the molecular constitution of the BT2 solution cannot be described as a simple combination of those characteristic for the individual B2 and T2 solutions in accordance with the Raman spectroscopic data (see Figure 2). To make the origin of these 91 and 188 ppm peaks unambiguously clear, an off-resonance ^{13}C NMR spectrum was measured and compared with another $^{13}C\{^1H\}$ NMR spectrum recorded with complete broadband decoupling of the protons (Figure 7). The off-resonance experiment is the most straightforward technique for distinguishing carbons in

$$-CH_3,\ -CH_2-,\ \begin{matrix}|\\-CH-\\|\end{matrix}\ \text{and}\ \begin{matrix}|\\-C-\\|\end{matrix}$$

fragments, since they respectively appear as quartets, triplets, doublets, and singlets in the off-resonance spectrum.[27] The immediate conclusion drawn from Figure 7 is therefore that the singlet peaks at 91 and 188 ppm in the off-resonance spectrum both originate from quaternary carbon atoms in CA. Taking into account the large value of these chemical shifts compared with the value of 77 ppm (corresponding to the quaternary alcoholic carbon of b in CA) and 178 ppm (corresponding to the carboxylic acid carbon of d in CA), respectively, the 91 and 188 ppm resonances can be almost utterly assigned to the corresponding quaternary carbons in CA with dissociation of the proton from the alcohol OH group, i.e., b′ and d′ carbon centers as described in Scheme 2.

Turning again back to Figure 6A, let us first focus our attention on the b, b_1, and b′ peaks appearing between 74 and 94 ppm. The integrated intensities of the individual (b + b_1) peaks relative to those of the reference (a + a_1) peak(s) remained almost unchanged (I(b+b_1)/I(a+a_1) = ∼0.5) within the experimental accuracy for the three spectra of parts a−c of Figure 6A, while the corresponding relative intensity of the (b + b_1) peaks for spectrum d of Figure 6A is approximately

(27) Martin, M. L.; Martin, G. J.; Delpuech, J.-J. *Practical NMR Spectroscopy*; Heyden & Son Ltd: London, 1980.

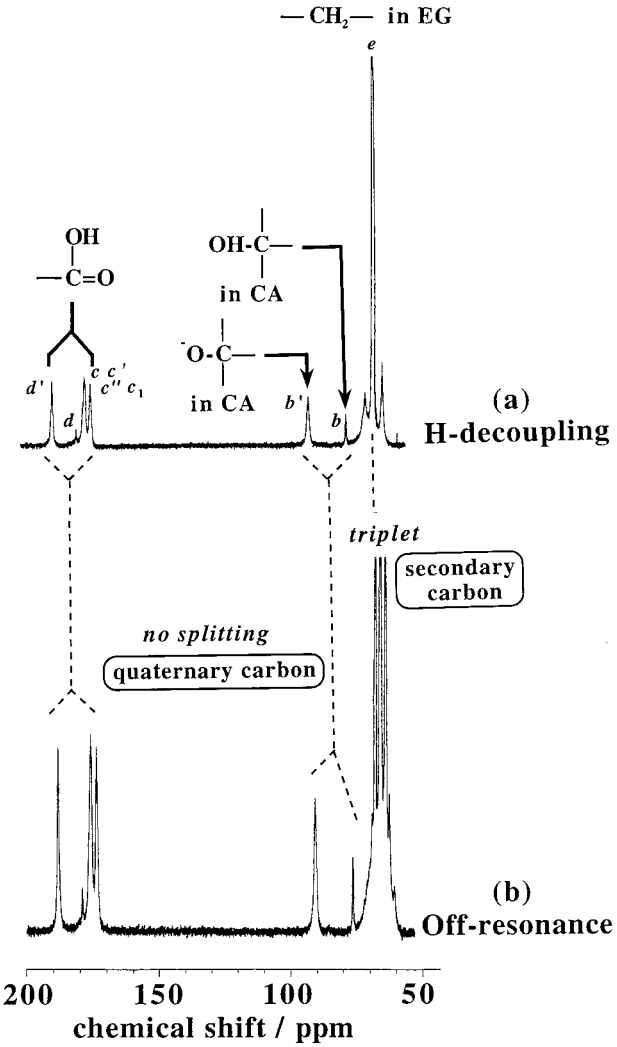

Figure 7. ^{13}C NMR spectra of BT3 solution with the molar ratio Ba/Ti/CA/EG = 0.3:0.3:1:4 recorded with (a) complete broadband decoupling of proton and (b) off-resonance. The peaks at 91 (b′) and 78 (b) ppm and peaks between 170 and 200 ppm remain unchanged as singlets, proving their origin to be the quaternary carbon in CA. The peak at 65 ppm (e) associated with the methylene carbon (secondary carbons; $-CH_2-$) in EG has split into three peaks in the off-resonance spectrum as expected.

Scheme 2

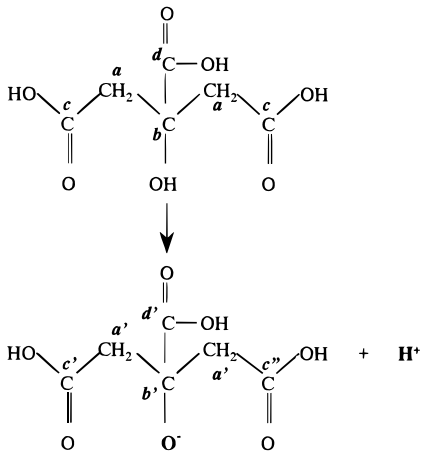

0.2, which is much smaller than 0.5 for the other three solutions. It is obvious that the observed decrement of the relative intensity of the (b + b_1) peaks in spectrum

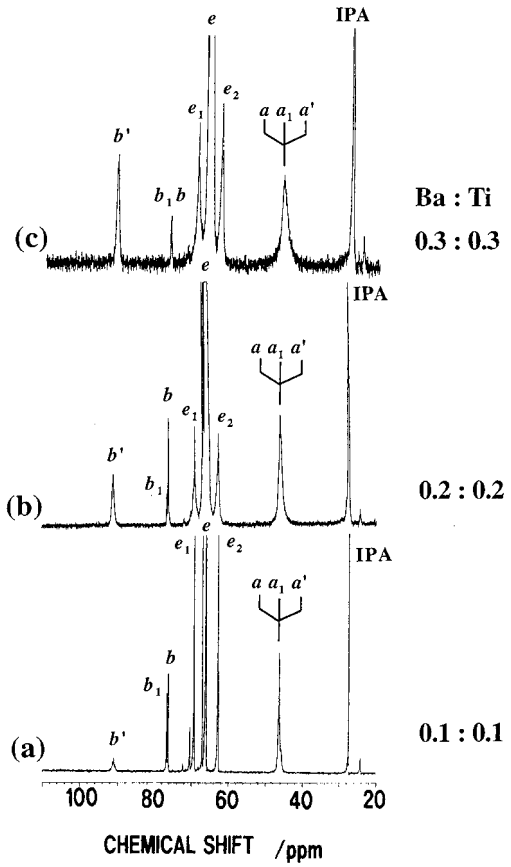

Figure 8. $^{13}C\{^1H\}$ NMR (decoupled) spectra in the region of 20−110 pm for various solutions with the molar ratio Ba/Ti/CA/EG = (a) 0.1:0.1:1:4 (BT1), (b) 0.2:0.2:1:4 (BT2), and (c) 0.3:0.3:1:4 (BT3). IPA stands for isopropyl alcohol. For definition of other symbols marked on peaks, see Schemes 1−3 as well as the text.

d of Figure 6A has arisen from the ionization described in Scheme 2, which is unique to the BT2 solution containing both Ba and Ti ions in equal amounts. Since the ionization described by Scheme 2 is never expected in solutions free from metals even at very high pH,[28−30] the $-C-O^-$ group responsible for the resonance at 91 ppm in spectrum d of Figure 6A should be present not as a free ion but as a ligand stabilized through complexation. The fact that the b′ peak has been observed exclusively in solutions containing both Ba and Ti ions implies formation of another type of complex different from those present in solutions as only Ba or Ti ions. Spectra a−c of Figure 8 respectively show $^{13}C\{^1H\}$ NMR (decoupled) spectra of BT1, BT2, and BT3 in the 20−110 ppm region. The intensity of the b′ peak relative to the (a + a_1+ a′) peak(s) is linearly increased with increasing metal concentration, indicating a linear increase in the amount of a given complex unique to these solutions. The most probable scenario for the complexation in solutions containing both Ba and Ti ions is that the simultaneous presence of Ba and Ti prompts rearrangement of CA to form a mixed-metal $BaTi-CA_n$ complex according to the following type of reaction (the

(28) Fujita, T. *Chem. Pharm. Bull.* **1982**, *30*, 3461.
(29) Strouse, J.; Layten, S. W.; Strouse, C. E. *J. Am. Chem. Soc.* **1977**, *99*, 562.
(30) Tananaeva, N. N.; Trunova, E. K.; Kostromina, N. A.; Shevchenko, Yu. B. *Teor. Eksp. Khim.* **1990**, *26*, 706.

charge for each chemical species is omitted for simplicity):

$$a\mathrm{Ba} + a\mathrm{Ti} + b\mathrm{CA} \rightarrow a[(\mathrm{BaTi})-(\mathrm{CA})_n] + (b - an)\mathrm{CA} \quad (2)$$

wherein only a 1:1 complex is taken into consideration. It is now quite probable that the resonance at 91 ppm for the b′ carbon center exclusively observed in solutions containing both Ba and Ti ions has come from formation of a mixed-metal CA complex like $BaTi-CA_n$. Similarly, the resonance at 188 ppm for the central carboxylic acid d′ carbon should be linked with formation of $BaTi-CA_n$. The magnetic resonance for the terminal carboxylic acid c carbon appears to be significantly modified upon the complexation, as indicated by the appearance of extra c′ and c″ peaks in spectrum d of Figure 6B. Although they are heavily overlapped with a lot of other neighboring peaks, the complete absence of such extra peaks in the three spectra of parts a−c of Figure 6B leads to the supposition that at least two types of magnetically nonequivalent terminal COOH groups will be involved in a given complex unique to the BT2 solution (spectrum d of Figure 6B). When the two terminal COOH groups of CA coordinate to Ba and Ti to form a mixed-metal CA complex, the two terminal carboxylic acid c′ and c″ carbons in Scheme 2 differ magnetically from each other, thereby giving rise to resonances with different chemical shifts as is indeed observed in spectrum d of Figure 6B. However, there still remains a fundamental question about the metal stoichiometry of the complex in question that is unresolved.

Our basic proposition is that the ratio of Ba to Ti in the proposed mixed-metal $BaTi-CA_n$ complex is just confined to 1:1 even when the initial Ba/Ti ratios in solution deviate from the stoichiometric value of 1. In other words, excess Ba or Ti will be stabilized with CA to form a single-metal Ba− or Ti−CA complex, and they do not disturb the formation of a mixed-metal 1:1 $BaTi-CA_n$ complex. According to this scheme, the molecular constitution in each of our samples can be approximately described as shown in the last column of Table 1. Of solutions listed in Table 1, B1T3, B2T3, B2T1, and B3T1 are of particular importance, since their Ba/Ti ratios are not equal to 1. If our basic proposition is correct, excess Ba or Ti in these solutions do not influence the magnitude of the b′ peak, since both the single-metal Ba− and Ti−CA complexes produce no resonance at 91 ppm characteristic for b′ carbon (see the ^{13}C NMR spectra of B2 and T2 shown in spectra b and c of Figure 6A, respectively). The results related to this concern are summarized in Figure 9, wherein c(b′) (the amount of b′ carbon of CA in Scheme 2**)**; i.e., it is proportional to the relative intensity of the b′ peak) is plotted against c(Ba) (the amount of Ba) for various solutions. c(b′) was evaluated from the total amount of CA and the value of R(b′)/(R(b+b_1) + R(b′)) determined experimentally from the ^{13}C NMR spectra, where R(b′) and R(b+b_1) stand for the respective integrated intensities of the b′ peak and of the (b+b_1) peaks relative to those of the reference (a+a_1+a′) peak(s). When c(Ba) is increased from 0 mol up to 0.3 mol, while the condition c(Ba) = c(Ti) is maintained, c(b′) is linearly increased (BT0 → BT1 → BT2 → BT3 in Figure 9). This indicates a linear increase in the amount of the mixed-metal

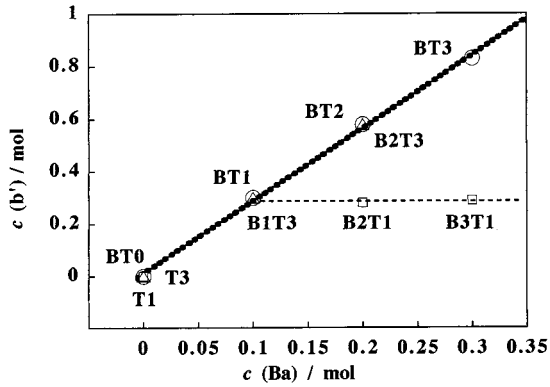

Figure 9. Plots of the amount of b′ carbon (see Scheme 2) in CA (c(b′)) against the amount of Ba (c(Ba)) for various solutions. Signs marked near the data points stand for solution numbers as defined in Table 1.

$BaTi-CA_n$ complex. In contrast, when c(Ti) is kept at a constant value of 0.1 mol, c(b′) is naturally increased to c(Ba) = 0.1 mol (T1 → BT1 in Figure 9), but a further increase in c(Ba) from 0.1 mol up to 0.3 mol does not increase the value of c(b′) (BT1 → B2T1 → B3T1 in Figure 9). This indicates that the amount of the mixed-metal $BaTi-CA_n$ complex in BT1, B2T1, and B3T1 remains almost unchanged, and the excess Ba in B2T1 and B3T1 does not seriously influence the metal stoichiometry of the coexisting mixed-metal $BaTi-CA_n$ complex. Note also in Figure 9 that c(b′) for B1T3 coincides with that for BT1 within experimental accuracy, and similarly, c(b′) for B2T3 is almost equal to that for BT2. This indicates that the excess Ti in B1T3 and B2T3 does not further enhance the deprotonation of CA in Scheme 2, and hence, the metal stoichiometry of the mixed-metal $BaTi-CA_n$ complex is not influenced by the excess Ti. In view of these observations, we conclude that the ratio of Ba to Ti in the proposed mixed-metal $BaTi-CA_n$ complex is very close to 1:1.

On the assumption that only CA with the b′ carbon participates in the formation of the mixed-metal $BaTi-CA_n$ complex, one can estimate how many CA (i.e., the value of "n" in the chemical formula) are incorporated into the mixed-metal complex from a variation of c(b′) as a function of c(Ba). When the complexation follows eq 2, c(b′) and c(b+b_1) (the amount of b and b_1 carbons in Scheme 1) should be, respectively, increased and decreased with increasing c(Ba) (i.e., "a" in eq 2) while keeping the total amount of CA (i.e., "b" in eq 2) constant. This has indeed been observed, as shown in Figure 10. A linear increase in c(b′) with c(Ba), which is accompanied by a linearly decreased c(b+b_1), thus indicates that the amount of the mixed-metal $BaTi-CA_n$ is linearly increased at the expense of free CA. The extrapolation of the linear c(b′) vs c(Ba) plot to c(Ba) = 1 mol gives the amount of CA participating in the formation of the mixed-metal $BaTi-CA_n$, and one can now have $n \doteqdot 3$.

(2) Characterization of a Mixed-Metal Ba−Ti Citric Acid Complex in the Solid State. *(a) Elemental Analysis and Thermal Decomposition of the Complex.* The ICP chemical analysis gave the ratio of Ba to Ti in the isolated BaTi-mixed CA complex to be 1.006 ± 0.009, meaning that the complex is of a stoichiometric compound with respect to the metal ratio within experimental accuracy. The chemical formula of the isolated

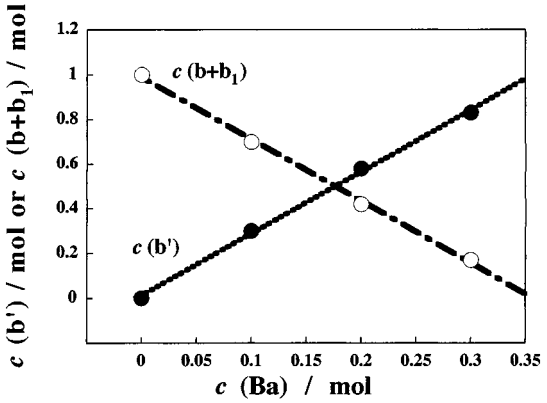

Figure 10. Plots of the amount of b′ or b + b_1 carbons in CA (c(b′) or c(b+b_1)) against the amount of Ba (c(Ba)) for BT0, BT1, BT2, and BT3 solutions with the respective molar ratio Ba/Ti/CA/EG = 0:0:1:4, 0.1:0.1:1:4, 0.2:0.2:1:4, and 0.3:0.3:1:4. For definition of b, b_1, and b′, see Scheme 2.

complex is then written as $BaTi(C_6H_{8-x}O_7)_y \cdot zH_2O$, where $C_6H_{8-x}O_7$ represents citric acid with dissociation of protons by x. The elemental analysis for C, H, and O involved in the complex gave C = 25.6%, H = 3.5%, and O = 48.5%, which suggests the composition of the complex to be best formulated as $BaTi(C_6H_6O_7)_3 \cdot 4H_2O$ by taking into account the electrical neutrality as well (i.e., the values of x, y, and z are 2, 3, and 4, respectively). The calculated values for this structure are C = 26.1%, H = 3.2%, and O = 48.3%, which are reasonably in agreement with the observed analytical results. The composition of the isolated complex is basically similar to those previously reported; e.g., $BaTi(C_6H_6O_7)_3 \cdot 6H_2O$[21] and $BaTiO(C_6H_6O_7)_2 \cdot C_6H_8O_7 \cdot 7H_2O$,[31] although the number of hydrated waters and the number of dissociated protons in CA differ from each other. Note that the number of CA coordinating to Ba and Ti (i.e., y = 3) coincides with that estimated from ^{13}C NMR spectroscopy for solutions as described in the previous section.

Figure 11a illustrates the TG and DTA curves of $BaTi(C_6H_6O_7)_3 \cdot 4H_2O$ heat-treated in static air using a heating rate of 40 °C/min in the temperature range 25−1000 °C. The corresponding evolution behavior of H_2O and CO_2 as a function of time and temperature, as determined by the mass spectrometry, is shown in Figure 11b. The thermal decomposition of $BaTi(C_6H_6O_7)_3 \cdot 4H_2O$ takes place in three major steps: (i) dehydration of the hydrated water (25−120 °C) to form $BaTi(C_6H_6O_7)_3$, (ii) decomposition of the unhydrated complex to form intermediate phases of, for example, $Ba_2Ti_2O_5 \cdot CO_3$ (120−600 °C), and (iii) the decomposition of intermediate phases to form $BaTiO_3$ (600−700 °C). The first TG weight loss of approximately 9.2% in the temperature range 25−120 °C with an endothermic peak at 95 °C (Figure 11a) is mainly due to the departure of four (theoretical weight loss 8.7%) water molecules from $BaTi(C_6H_6O_7)_3 \cdot 4H_2O$. This is supported by the mass spectroscopic analysis shown in Figure 11b, wherein only water (with a mass of 18) evolution was observed up to 150 °C. The subsequent thermal decomposition of the unhydrated $BaTi(C_6H_6O_7)_3$ in the range 120−600 °C is very complicated, and the DTA shows three main

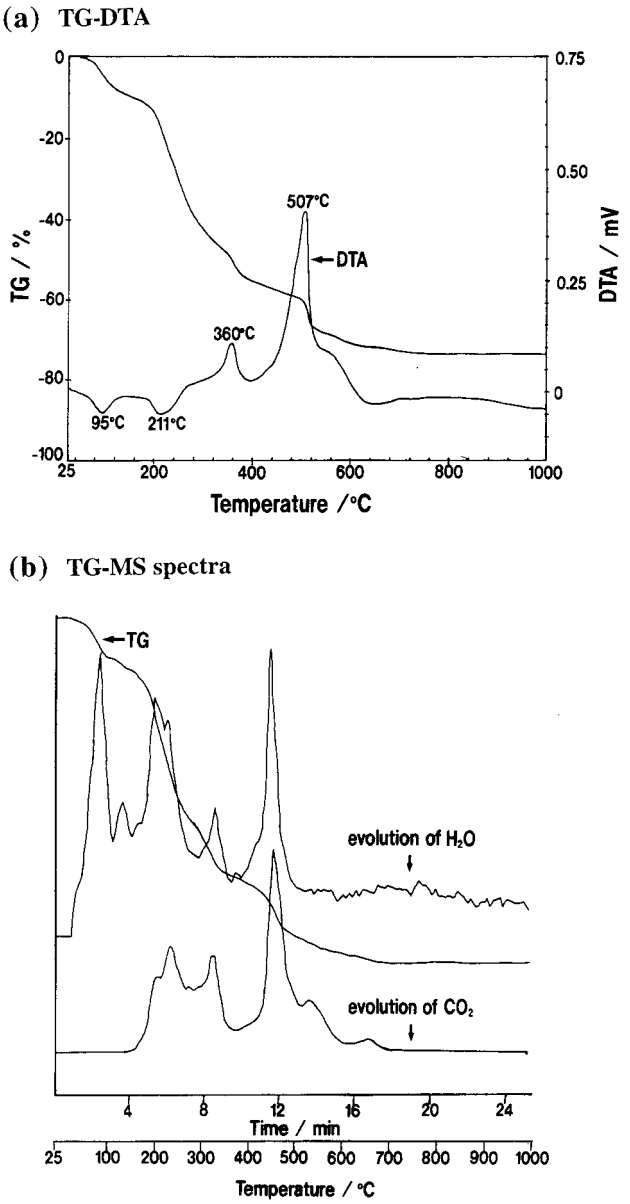

Figure 11. (a) TG-DTA curves and (b) H_2O/CO_2 evolution behavior (TG-MS) of $BaTi(C_6H_6O_7)_3 \cdot 4H_2O$ heat-treated in air at a heating rate of 40 °C/min in the temperature range 25−1000 °C.

thermal events, an endotherm at 211 °C, an exotherm at 360 °C, and an intense exotherm at 507 °C, all these being accompanied by evolution of both H_2O and CO_2 (Figure 11b). The basic decomposition scheme may be nearly the same as those described in ref 31 or ref 21, i.e., the endotherm at 211 °C being related to the formation of BaTi−itaconate ($BaTi(C_5H_4O_4)_3$) through BaTi−aconitate ($BaTi(C_6H_4O_6)_3$), the exotherm at 360 °C to the partial combustion of the BaTi−itaconate with the probable formation of $BaTiO(C_5H_4O_4)_{2-x}(CO_3)_x$, and the last exotherm at 507 °C to the combustion of $BaTiO(C_5H_4O_4)_{2-x}(CO_3)_x$ with the probable formation of $Ba_2Ti_2O_5 \cdot CO_3$ or related carbonates having different stoichiometries. The formation of $Ba_2Ti_2O_5 \cdot CO_3$ as an intermediate may be supported by the fact that a small TG weight loss of 2.7% in the temperature range 640−700 °C is in good agreement with the theoretical loss of

(31) Rajendran, M.; Subba Rao, M. *J. Solid State Chem.* **1994**, *113*, 239.

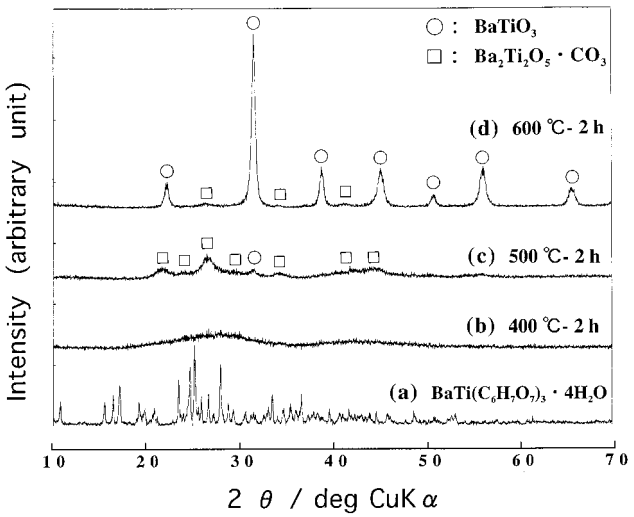

Figure 12. X-ray diffraction patterns of (a) $BaTi(C_6H_6O_7)_3 \cdot 4H_2O$ and of its decomposition products in static air for 2 h at (b) 400 °C, (c) 500 °C, and (d) 600 °C.

2.65% calculated according to the following reaction:

$$Ba_2Ti_2O_5 \cdot CO_3 \rightarrow 2BaTiO_3 + CO_2 \qquad (3)$$

Mass spectrometry confirmed the evolution of CO_2 in the temperature range 600−700 °C (Figure 11b). It should, however, be mentioned that the weight-loss agreement does not necessarily mean that the composition of intermediate phases can be fixed. The reaction product just after the exotherm at 507 °C will therefore be better described as a mixture of several intermediate phases coexisting in different concentrations. There is no substantial thermal event above 700 °C, and at this temperature the weight has been lost by 72.5%. The theoretical weight loss in the case of complete conversion from $BaTi(C_6H_6O_7)_3 \cdot 4H_2O$ to $BaTiO_3$ ought to be 71.8%.

A progressive formation of $BaTiO_3$ from the thermal decomposition of $BaTi(C_6H_6O_7)_3 \cdot 4H_2O$ was traced with XRD, as shown in Figure 12. The product after the heat treatment at 400 °C for 2 h was primarily amorphous in structure, as shown by the broad continuum in the XRD pattern in Figure 12b. Broad peaks showed up after the heat treatment at 500 °C for 2 h, the positions of which agree with those for $Ba_2Ti_2O_5 \cdot CO_3$ previously reported.[13,16] Note, however, that we cannnot completely exclude the possibility that a broad, weak peak near $2\theta = 24$ ° also corresponds to microcrystalline barium carbonate. Formation of such microcrystalline barium carbonate has been indeed confirmed in sol-precipitation synthesis of barium titanate and barium zirconate.[32−35] The heat treatment at 600 °C for 2 h resulted in formation of $BaTiO_3$ as a major phase, but reflections characteristic for $Ba_2Ti_2O_5 \cdot CO_3$ (and/or microcrystalline barium carbonate) still persist as minor components (Figure 12d). In agreement with the TG-DTA analysis (Figure 11a), the complete conversion to $BaTiO_3$ was achieved after the heat treatment at 700 °C for 2 h (not shown here). Formation of $Ba_2Ti_2O_5 \cdot CO_3$ is also known in the Pechini-type PC processing for $BaTiO_3$,[13,16] and reported XRD patterns for its decomposition products at temperatures between 500 and 600 °C almost mimic what has been observed in this study (spectra c and d of Figure 12).

(b) Possible Model of the Structure of the Complex Inferred from Raman and Solid-State ^{13}C NMR Spectroscopic Data. Figure 13 represents our proposed model for the structure of $BaTi(C_6H_6O_7)_3$, in which the position of each atom has been optimized by a molecular mechanics calculation. It displays six-coordinated titanium and barium centers, and the salient feature of the CA ligand is its tridentate nature as a whole molecule, thus forming a fused six-membered chelate ring. Basic assumptions with respect to the coordination of CA ligands to Ba and Ti in doing the calculation include the following.

(A1) Three carboxylic acid −COOH groups of each CA are not dissociated to form carboxylate −COO− anions, although one of them should be deprotonated from the chemical formula. This is just because we cannot specify which of the three −COOH groups is deprotonated.

(A2) Only the two terminal carboxylic acid −COOH groups of each CA are involved in the complexation, while the central carboxylic acid −COOH group does not participate in the complexation.

(A3) Dissociation of a proton occurs in the alcohol OH group of each CA, and the resulting alkoxide group of $C-O^-$ coordinates simultaneously to Ba and Ti.

For the sake of clarity, we give Scheme 3, showing schematically how one of CA coordinates to both Ba and Ti. Ba and Ti atoms are bridged by one alkoxide oxygen atom of the fully deprotonated CA ligand, and the two terminal carboxylic acid −COOH groups coordinate in a monodentate fashion either to Ba or to Ti, thus forming a fused six-membered chelate ring. The remaining central carboxylic acid −COOH group is noncoordinating. We have strong evidence for assumptions A1−A3, which have been inferred from Raman and solid-state ^{13}C NMR spectroscopy, as shown below.

Figure 14b shows a Raman spectrum of $BaTi(C_6H_6O_7)_3 \cdot 4H_2O$, which is compared with a reference Raman spectrum of anhydrous CA (Figure 14a). Also included for the purpose of a comparison is the solution Raman spectrum of BT3 (Figure 14c) (an CA/EG solution containing both Ba and Ti with a molar ratio of Ba/Ti/CA/EG = 0.3:0.3:1:4). A recent ab initio study on ground-state vibrations of CA should be used as an excellent basis for interpreting our Raman spectrum of $BaTi(C_6H_6O_7)_3 \cdot 4H_2O$.[26] Despite that the Raman spectrum of the mixed-metal complex is extremely complicated, there will be several important regions of spectroscopic interest, which involve the −C═O (in COOH), −C−OH (carbon bonding to the alcoholic OH), Ti−O, and Ba−O bonding regions with respective vibrational features occurring in the ranges 1500−1800, 900−1000, 500−700, and 200−400 cm^{-1}.

The two rather strong and sharp peaks at 1739 and 1700 cm^{-1} in anhydrous CA (Figure 14a) can be, respectively, assigned to the central carboxyl ν(C═O) stretching and the terminal carboxyl ν(C═O) stretching modes.[26] It is predicted by ab initio calculations on CA[26] that there is an intramolecular hydrogen bond between the alcoholic hydrogen and one of the terminal carboxyl oxygens, as is schematically shown in Scheme 4.

(32) Phule, P. P.; Risbud, S. H. *J. Mater. Sci.* **1990**, *25*, 1169.
(33) Phule, P. P.; Khairulla, F. *Ceram. Trans.* **1990**, *12*, 725.
(34) Phule, P. P.; Risbud, S. H. *Adv. Ceram. Mater.* **1988**, *3*, 183.
(35) Phule, P. P.; Risbud, S. H. *Mater. Sci. Eng.* **1988**, *B3*, 241.

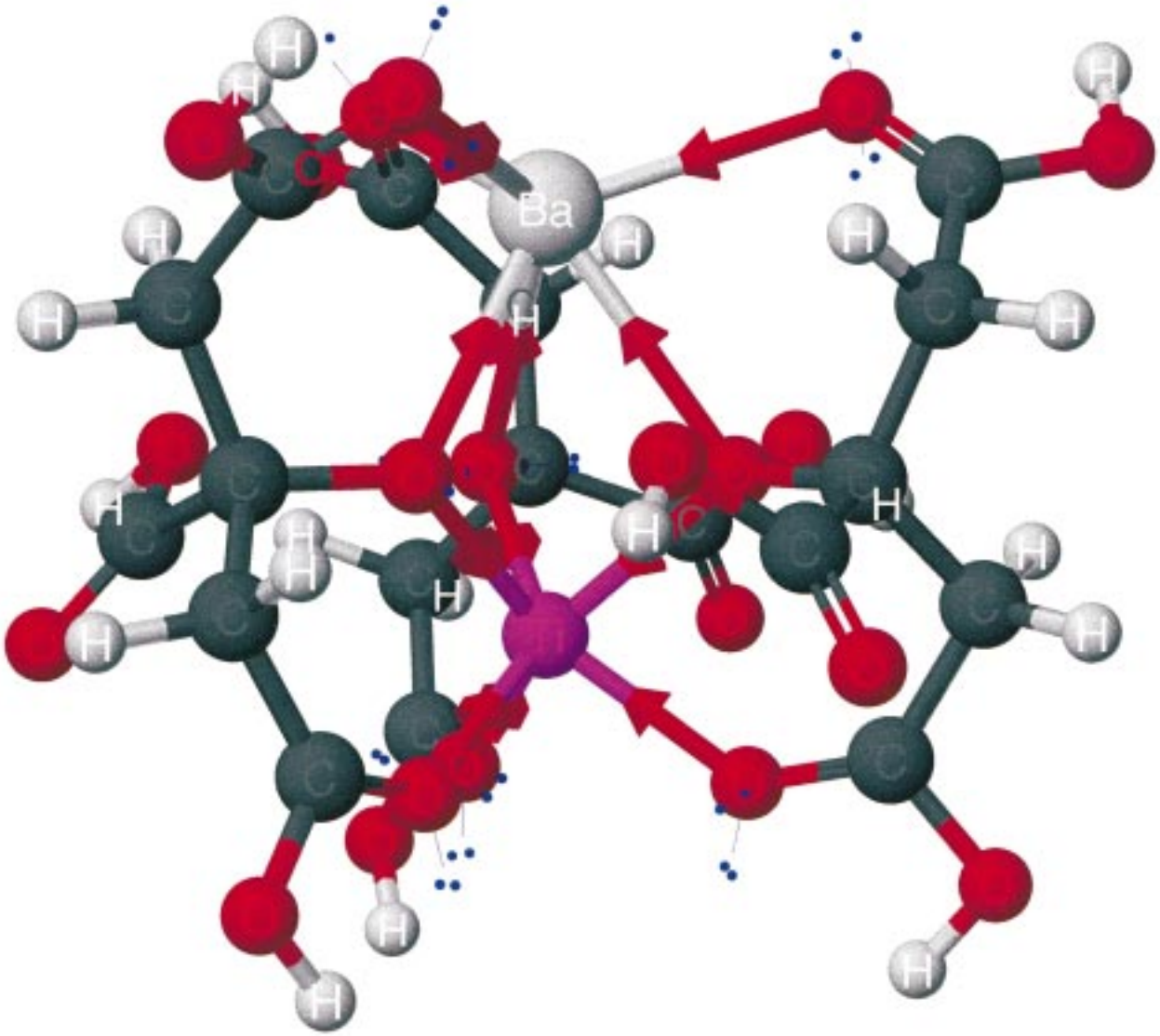

Figure 13. Proposed model for the structure of $BaTi(C_6H_6O_7)_3$ species.

Scheme 3

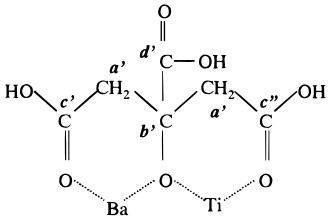

The involvement of the alcoholic hydrogen in the formation of an intramolecular hydrogen bond lowers the $\nu(C^2{=}O)$ frequency so that a relatively broad feature around 1630 cm^{-1} in Figure 14a is attributable to the stretching vibration associated with the second terminal carboxyl $C^2{=}O$ bond with the intramolecular hydrogen bond. Although the first terminal carboxyl $\nu(C^1{=}O)$ mode has shifted 70 cm^{-1} from 1700 to 1630 cm^{-1} upon the complexation of CA with Ba and Ti ($\nu(C^1{=}O) \rightarrow \nu(C^{c'}{=}O)$), a shift of only 40 cm^{-1} has been observed for the second terminal carboxyl $\nu(C^2{=}O)$ mode ($\nu(C^2{=}O) \rightarrow \nu(C^{c''}{=}O)$; Figure 14b). However, the lower degree of shift in the latter would be a make-believe. This is because the second terminal carboxyl $C^2{=}O$ is first involved in the formation of an intramolecular hydrogen bond in CA, which was the reason for the lower value of its Raman shift (1630 cm^{-1}) compared with the first carboxyl $\nu(C^1{=}O)$ frequency of 1700 cm^{-1}, and the observed 40 cm^{-1} shift on going from CA to the mixed-metal complex would be too big for the second terminal carboxyl $C^2{=}O$ to maintain the intramolecular hydrogen bond if it is not coordinated to any metals. Since the second terminal carboxyl $C^2{=}O$ will not be able to participate simultaneously in the formation of the intramolecular hydrogen bond and the formation of a metal−oxygen bond, it is likely that the initially formed intramolecular hydrogen bond between the alcoholic hydrogen and the second terminal carboxyl oxygen in CA is completely broken, instead of which a new strong metal−oxygen bond forms in $BaTi(C_6H_6O_7)_3{\cdot}4H_2O$ as described in Scheme 3. According to this consideration, the net value of the shift upon the complexation for the second terminal carboxyl $\nu(C^2{=}O)$ mode should be 110 cm^{-1} from 1700 to 1590 cm^{-1} rather than 40 cm^{-1} from 1630 to 1590 cm^{-1}, the net shift of 110 cm^{-1} being even larger than 70 cm^{-1} for the first terminal carboxyl $\nu(C^1{=}O)$ mode, which suggests that the second terminal carboxyl $C^2{=}O$ coordinates to Ti^{4+} with a higher valency (rather than Ba^{2+} with a lower valency) to form a

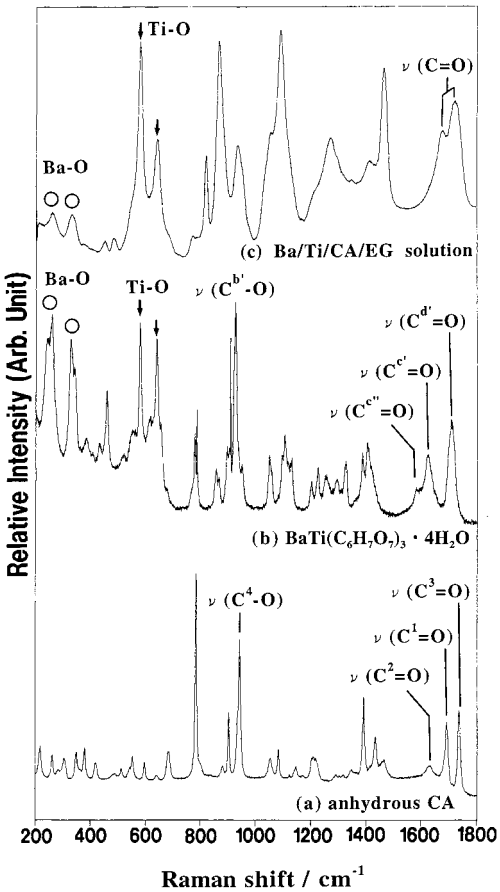

Figure 14. Raman spectra of (a) anhydrous citric acid, (b) $BaTi(C_6H_6O_7)_3{\cdot}4H_2O$, and (c) BT3 solution with the molar ratio Ba/Ti/CA/EG = 0.3:0.3:1:4. Symbols of Ti−O and Ba−O stand for stretching vibrations between the oxygen and each metal. C═O and C−O respectively stand for carboxyl C═O stretching modes and C−O stretching vibrations in C−OH including the alcohol OH group. For signs attached to carbons, see Schemes 3 and 4.

Scheme 4

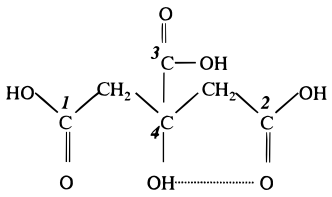

stronger bond between Ti^{4+} and O, thus weakening the bond strength of C^2═O. On the other hand, the central carboxyl $\nu(C^3{=}O)$ mode has shifted only 30 cm^{-1} from 1739 to 1709 cm^{-1} upon the formation of $BaTi(C_6H_6O_7)_3{\cdot}4H_2O$ ($\nu(C^3{=}O) \rightarrow \nu(C^{d'}{=}O)$; Figure 14b), suggesting that the central carboxyl C^3═O does not coordinate to any metal. In view of these considerations, we propose that the first and the second terminal COOH groups of each CA in $BaTi(C_6H_6O_7)_3{\cdot}4H_2O$, respectively, coordinate to Ba and Ti, and the central COOH group of each CA is not coordinating (i.e., assumption A2).

The strong peak at 940 cm^{-1} in anhydrous CA (Figure 14a) can be assigned to the C^4−O stretching vibration in −C^4−OH, including the alcohol OH group,[26] and it underwent a 20 cm^{-1} shift to 920 cm^{-1} upon the complexation ($\nu(C^4{-}O) \rightarrow \nu(C^{b'}{-}O)$). Although this lower frequency shift suggests the formation of metal−oxygen bonding through the alcohol OH group in CA, it is not possible to conclude solely from this Raman data if the proton is really dissociated from the alcohol OH. Evidence for such a deprotonation from the alcohol OH will be obtained from solid-state ^{13}C NMR spectroscopy as shown later (see Figure 15b).

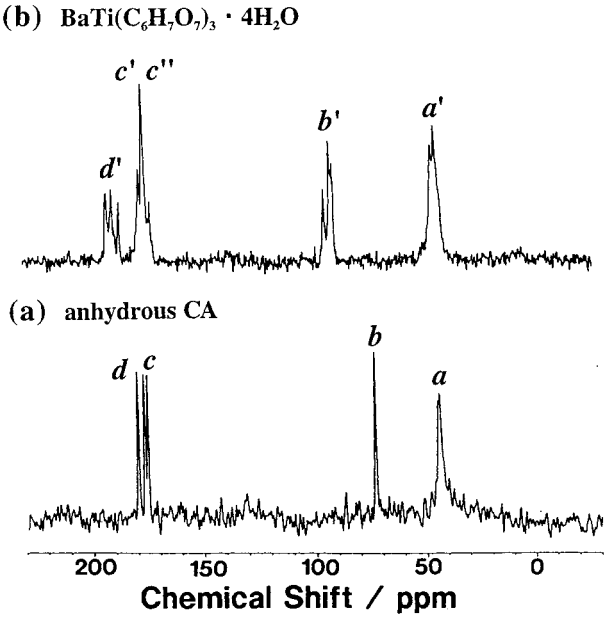

Figure 15. Solid-state ^{13}C NMR of (a) anhydrous citric acid and (b) $BaTi(C_6H_6O_7)_3{\cdot}4H_2O$. For definition of symbols marked on peaks, see Schemes 1 and 3.

A comparison of the Raman spectrum of the anhydrous CA (Figure 14a) with that (Figure 14b) of $BaTi(C_6H_6O_7)_3{\cdot}4H_2O$ in frequencies below 700 cm^{-1} provides information on metal−oxygen stretching vibrations. A characteristic doublet at 580 and 630 cm^{-1} (marked with arrows), which is absent in the Raman spectrum of CA, can be assigned, respectively, to the symmetric and antisymmetric Ti−O stretching vibrations.[16,24] Owing to the large mass difference between Ti and Ba, another characteristic feature showing up as a strong doublet at 260 and 330 cm^{-1} upon the complexation can be assigned to stretching vibrations associated with Ba−O bonds (marked with ○). These two characteristic doublets are similarly observed in the Raman spectrum of the BT3 solution containing 0.3 mol of Ba and Ti for each relative to 1 mol of CA (Figure 14c), suggesting that the basic environment around the Ba−O and Ti−O bonds in the mixed-metal complex is preserved also in solutions.

Solid-state ^{13}C NMR spectra of anhydrous CA and $BaTi(C_6H_6O_7)_3{\cdot}4H_2O$ are shown in parts a and b of Figure 15, respectively. The assignment for each peak in the spectrum of the anhydrous CA is straightforward, the resonances at 46 and 73 ppm corresponding to the methylene carbon a and the alcoholic carbon b (as described in Scheme 1), respectively, the peak at 188 ppm showing a resonance at the lowest magnetic field to the central carboxylic acid carbon d, and the two terminal carboxylic acid carbons c splitting into two components at 176 and 178 ppm owing to the slight difference of their magnetic environments in the solid.[36] An inspection of the alcoholic carbon b region for the

(36) Johnson, L. F.; Jankowski, W. C. *Carbon-13 NMR Spectra*; Wiley: New York, 1972.

spectrum of $BaTi(C_6H_6O_7)_3 \cdot 4H_2O$ shows the complete absence of the resonance at 73 ppm characteristic of the alcoholic carbon b instead of which a new triplet shows up in the region of 90 ppm. This observation, in agreement with our conclusion derived from the solution-state ^{13}C NMR spectroscopy, indicates that the alcohol OH in CA is fully deprotonated to form an alkoxide oxygen atom, building together with two terminal carboxyl C═O groups a fused six-membered chelate ring as described in Scheme 3 (i.e., assumption A3). The magnetic environment for each of alkoxide b′ carbons in the three coordinating CA slightly differs from each other, which leads to the observation of the triplet at ∼90 ppm. A similar characteristic triplet, which has been observed for $BaTi(C_6H_6O_7)_3 \cdot 4H_2O$ at the lowest magnetic field region of 190−200 ppm, comes from the three d′ carboxylic acid carbons with three magnetically different environments each directly bonded to the respective b′ alkoxide carbon.

Conclusion

The Raman and ^{13}C NMR spectra of the Ba/Ti/CA/EG precursor solutions indicated formation of a mixed-metal CA complex with a stoichiometry close to Ba/Ti/CA = 1:1:3, in which both barium and titanium ions were simultaneously stabilized with CA. There was strong ^{13}C NMR spectroscopic evidence for the presence of an alkoxide oxygen atom generated as a result of deprotonation of the alcohol OH group in CA. The Raman spectrum of an isolated complex of $BaTi(C_6H_6O_7)_3 \cdot 4H_2O$ indicated that the two terminal COOH groups of each CA coordinated in a monodentate fashion either to Ba or to Ti, while the central COOH group did not participate in coordination. The solid-state ^{13}C NMR spectrum of the same complex showed evidence that the alcohol OH in CA was fully deprotonated to form an alkoxide oxygen atom. This alkoxide oxygen atom played a major role in forming a mixed-metal complex, in which three fused six-membered chelate rings existed to stabilize this compound. The basic environment around the Ba−O and Ti−O bonds in the mixed-metal complex also seemed to be preserved in solution.

Acknowledgment. Financial support by “Research for the Future” Program No. JSPS-RFTF96R06901 from The Japan Society for the Promotion of Science is greatly acknowledged.

CM9806681